

Adsorption and Desorption of CO₂ on Korean Coal under Subcritical to Supercritical Conditions

Junwei He,[†] Yao Shi,[†] Sol Ahn,[†] Jeong Won Kang,[‡] and Chang-Ha Lee*,[†]

Department of Chemical and Biomolecular Engineering, Yonsei University, Seoul, Korea, Department of Chemical & Biological Engineering, Korea University, Seoul, Korea

Received: December 10, 2009; Revised Manuscript Received: January 30, 2010

Coal seams have been reported as possible storage sites for CO₂ to help mediate the global greenhouse gas problem. The adsorption and desorption characteristics of CO₂ on dry and wet (3.64 wt %) Korean coal (Kyungdong, anthracite coal) were studied using a static volumetric method at 298 and 318 K, and up to 150 atm. The adsorption of CO₂ was favorable at low temperatures and dry coal conditions. The hysteresis of coal swelling through adsorption, desorption, and readsorption of CO₂ was observed at subcritical condition. Hysteresis between adsorption and desorption isotherms occurred in both dry and wet coals. The crossover between adsorption and desorption isotherms in dry coal was observed near the critical region, while the excess amount of adsorbed CO₂ on wet coal was lower during desorption than during adsorption. Structural variations of the coal after the wet experiment were significant compared to those in the dry coal. In wet coal, the dissolution of H₂O in the CO₂ phase, absorption of CO₂ in the aqueous phase, and coal structure changes affected the estimation of adsorption amount, especially under supercritical condition.

1. Introduction

The excessive presence of CO₂ in the atmosphere is widely accepted as the main reason for global warming. Over the last several years, the most successful ways to geologically store captured carbon dioxide have been tested in depleted oil and gas fields, deep saline aquifers, and coal seams. Compared to both depleted oil and gas fields and deep saline aquifers, the mechanism of storing CO₂ in coal seams mainly depends on the adsorption properties of the porous coal structures.¹

Economically, some of coal seams may be infeasible for mining due to inadequate coal seam thickness, poor continuity of the area, or adverse geology. However, under the proper conditions, these coal seams can provide adequate sites for CO₂ storage. In addition to the sequestration of CO₂, this technology can also contribute to enhanced coal-bed CH₄ (ECBM) due to the competitive adsorption of the two gases.²

Because the temperatures of potential coal seam reservoirs typically range from 300–325 K and the depths of the coal seams are greater than 756 m, CO₂ sequestration occurs at supercritical condition ($T_c = 304$ K, $P_c = 73$ atm).³ As such, many physical properties, such as density, diffusivity, and viscosity, dramatically change near this critical point of CO₂, which affect the adsorption behavior under the supercritical condition.^{4–6} Therefore, it is very important to understand the adsorption mechanism of supercritical CO₂ on coal during CO₂ sequestration.

Recently, the adsorption of CO₂ onto bituminous coal has been widely studied.^{7–14} It has been reported that the CO₂ is stored in the dry coal seam in three different forms: adsorbed on the surface, dissolved in the coal matrix and as a free gas in the pores and fractures.⁹ As in the case of a polymer, coal is absorbing the CO₂, causing the coal to swell. Therefore, the uptake process of CO₂ can be viewed as a combination of adsorption on the coal's surface and penetration (absorption)

into the coal's matrix.¹⁰ And research has shown that the porous matrix of coal remained unchanged after the exposure to CO₂ at pressures up to 200 bar,¹¹ indicating that the observed swelling might be reversible. Also, it has been demonstrated that coal swelling could reduce the permeability of CO₂^{10,12–14} since swelling is known to change the void volume of coal seams.

Coal seams in Korea consist mainly of anthracite coal, which is a hard, compact variety of mineral coal that has a high luster and a lower calorific content than those of bituminous coal. Therefore, understanding the adsorption mechanism of CO₂ on anthracite coal is important for storing CO₂ in Korean coal seams. Moreover, once high pressure CO₂ is stored, it can spread through the coal seam or into other geological strata through permeation. As another possibility, stored CO₂ can leak from the coal seams over the long term. In both these cases, a decrease in stored CO₂ pressure results; therefore, it is important to understand the desorption mechanism of CO₂ from coal by depressurization.

In this study, the adsorption/desorption isotherms of CO₂ on both dry and wet Korean coals (Kyungdong coal) were measured under subcritical to supercritical conditions. The isotherm at 298 K was measured up to the saturation pressure of CO₂. At 318 K, the experimental pressure was extended to 150 atm. The desorption isotherm was measured by depressurizing CO₂ from 150 atm. Results from both the wet and dry coals were compared to each other, and the swelling structure variation, which stemmed from the adsorption/desorption of high pressure CO₂, was analyzed.

2. Experimental Section

2.1. Adsorbent. In this study, Kyungdong coal (anthracite coal, South Korea) was used as an adsorbent. The surface texture of the coal was visualized by microphotometry using an orthoplan microscope. Figure 1 shows that the cracks, which were micrometers in size, were well developed. Composition analysis results are given in Table 1. Kyungdong coal mainly consisted of vitrinite (88.5 wt %) and contained high amounts

[†] Yonsei University.

[‡] Korea University.

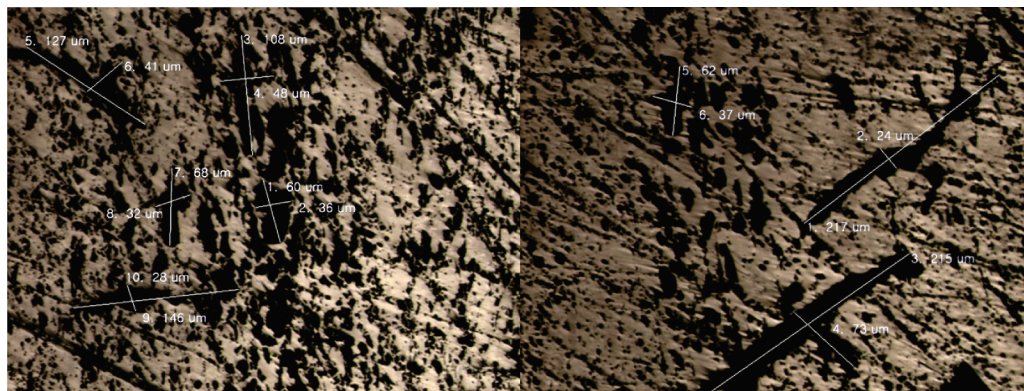


Figure 1. Texture images of Kyungdong coal taken by microphotometer with orthoplan microscope.

TABLE 1: Composition Analysis of Kyungdong Coal

sample name	moisture (wt %)	volatile (wt %)	ash (wt %)	fixed carbon (wt %)	<i>Q</i> (kcal/kg)	vitrinite reflectance (%)	vitrinite (wt %)	inertinite (wt %)	mineral (wt %)
Kyungdong coal	6.94	5.01	30.66	57.39	3980	5.07	88.5	5	6.5

of ash (30.66%), amounts significantly different from those of bituminous coals.^{7–14}

2.2. Experimental Apparatus. In this study, a volumetric method was used to measure the adsorption/desorption isotherms.¹⁴ A schematic diagram of the apparatus is shown in Figure 2. The system was composed of two main parts, an adsorption cell (642.6 mL) and a loading cell (411.4 mL). The pressure at each cell was measured by an electrical pressure transducer (Heise gauge, 901B) which had uncertainty in the total span of $\pm 0.035\%$. Cells with connecting lines and valves were immersed in a circulating water bath with a glass window and a PID controller. The lines that were exposed to air were wrapped with heating tape controlled by a PID controller. The temperature of each cell was measured using resistance temperature detectors (RTD, Pt 100 Ω), which were installed inside each cell and had an uncertainty of ± 0.1 K (Omega DP41-B). The RTDs were calibrated using a standard thermometer, and the adsorption and loading cell temperatures were maintained within ± 0.1 K.

A leakage test of the system was performed using high purity He (99.99%) at 200 atm and 353 K. The swelling of coal was observed using a window cell immersed in the water bath.

2.3. Experimental Method for Adsorption/Desorption. The free volume (void volume) of the adsorption cell excluding adsorbents was measured at room temperature using helium (He; 99.99%). Using the mass balances between the loading and

adsorption cells, the void volume (V_v) was calculated using the following equation:¹⁵

$$\left. \frac{P_l V_l}{Z_l R T_l} \right|_1 + \left. \frac{P_a V_v}{Z_a R T_a} \right|_1 = \left. \frac{P_l V_l}{Z_l R T_l} \right|_2 + \left. \frac{P_a V_v}{Z_a R T_a} \right|_2 \quad (1)$$

where P is pressure (Pa), T is temperature (K), V is volume (m^3), Z is the compressibility factor of CO₂, and R is the gas constant ($J \cdot mol^{-1} \cdot K^{-1}$). The subscripts l and a indicate the loading and adsorption cells, and the subscripts 1 and 2 indicate the initial and final states, respectively.

Z can be calculated from the following corresponding state correlation:¹⁶

$$Z = 1 + \left(0.083 - \frac{0.422}{T_r^{1.6}} \right) \frac{P_r}{T_r} + \omega \left(0.139 - \frac{0.172}{T_r^{4.2}} \right) \frac{P_r}{T_r} \quad (2)$$

where P_r is the reduced pressure, T_r is the reduced temperature, and ω is the acentric factor.

The fresh coal, delivered from the Kyungdong minefield, was dried overnight in a vacuum oven at 378 K. The adsorption experiments on dry coal were carried out at subcritical (298 K) and supercritical (318 K) temperatures. Before each dry coal experiment, the system was purged with He and evacuated for 2 h using a vacuum pump.

To prepare the wet coal, an excess amount of distilled water was added to the dry coal. After the wet coal was placed in a vacuum oven at 323 K, its mass change was periodically measured to control the amount of water in the coal. After the wet coal was placed into the adsorption cell at ~ 278 K, the same He purge method as above was applied to the system. The mass of wet coal in the adsorption cell was measured again after the system was evacuated for 30 min to minimize the loss of moisture from the coal. After the He purge, the mass of coal was measured again. The amount of water in the coal was calculated on the basis of the final mass change from that of the dry coal (3.64 wt %).

For the adsorption experiment, CO₂ (99.99%) from the loading cell was supplied to the adsorption cell. After equilibrium was reached, the pressure and temperature in each cell

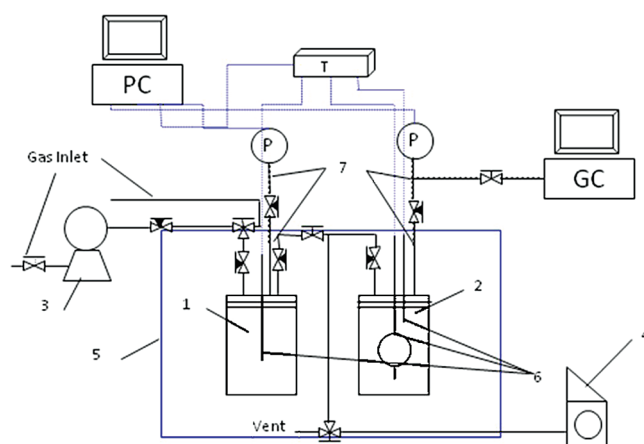


Figure 2. Schematic of adsorption experimental system.

were measured. The desorption experiment was carried out in reverse order from that explained above. The experiment reached equilibrium after 3 to 8 h, depending on the experimental conditions.

The excess adsorbed CO₂ was calculated using the following equation:

$$\rho_l V_l|_1 + \rho_a V_v|_1 = \rho_l V_l|_2 + \rho_a V_v|_2 + n^e m \quad (3)$$

where ρ is the density of CO₂ (mol/L), n^e is the (Gibbs) excess adsorbed CO₂ (mmol/g), m is the mass of coal (g), and V_v is the void volume in the adsorption cell (mL).

The density of CO₂ at the given T and P were obtained from the NIST Web site.¹⁷

2.4. Measurement of Coal Swelling. To determine the degree of coal swelling, pictures were taken with a digital camera (Nikon D200) through the adsorption cell view window. A dry coal plate was placed onto a reference sample (steel block) the shape of which did not change during the experiment. Pictures were taken after 20 h under each condition. The pixels of the coal plate and of the reference steel block were counted.

A dry coal plate (diameter = 13 mm) was placed onto a reference sample (steel block), the shape of which did not change during the experiment. Pictures were taken after 20 h under each condition through a high pressure view window (diameter = 25 mm). Coal swelling can be anisotropic;¹³ however, the coal plate in this study was composed of such small coal particles (150–500 μm) that the swelling was much more likely to be isotropic.⁹

The swelling ratio was calculated by the following equation:

$$\varphi = \left[\left(\frac{d_2}{d_1} \right) - 1 \right] \quad (4)$$

where φ is the diameter swelling ratio, d_1 is the initial diameter of the coal plate, and d_2 is the diameter of the coal plate at certain pressure.

The volume-swelling ratio (Ψ) can be calculated from the following equation:

$$\psi = \left(\frac{d_2}{d_1} \right)^3 - 1 \quad (5)$$

3. Theory

At supercritical condition, adsorption isotherms exhibit non-Langmuir behavior.^{5,6} Various adsorption models and correlations on coals have been suggested, including Toth,¹⁸ Dubinin–Astakhov,¹⁹ Dubinin–Radushkevich,^{2,7,8,20} simplified local density,^{21,22} two-dimensional Zhou–Gasem–Robinson equation of state,²³ and the lattice density functional theory model.²⁴

In this study, the experimental isotherm data were fitted using the Dubinin–Radushkevich (DR) equation with gas density rather than pressure because density is more meaningful at supercritical condition. In the following modified DR (M-DR) equation, pressure terms in the traditional DR equation were substituted with density terms:^{7,8}

$$n^e = n^0(1 - \rho/\rho^a) \exp\left[-D\left\{\ln\left(\frac{\rho^a}{\rho}\right)\right\}^2\right] \quad (6)$$

where n^0 is the adsorption capacity (mmol/g), D is the constant related to the affinity of the sorbent for the gas, and ρ^a is the adsorbed phase density (mol/L).

To consider the swelling effect on the isotherm, the following M-DR+k equation with the swelling parameter (k) was suggested:¹³

$$n^e = n^0(1 - \rho/\rho^a) \exp\left[-D\left\{\ln\left(\frac{\rho^a}{\rho}\right)\right\}^2\right] + k\rho(1 - \rho/\rho^a) \quad (7)$$

In the M-DR or M-DR+k equations, the adsorbed phase density of CO₂ must be predetermined. The density of the adsorbed phase should be determined using an adsorbent with no swelling or absorption. It has been reported that activated carbon may be an ideal material for determining the adsorbed phase density. The adsorbed phase density of activated carbon at 318 K and a zero Gibbs excess was reported to be 22.6 mol/L,²¹ and this value has been successfully applied to previously published works on coal adsorption.^{7,8,19} In this study, it was also assumed that the adsorbed phase density would be 22.6 mol/L, and the value did not change across the experimental range. This approximation implies the state of adsorption limit from the Gibbs definition of adsorption.²⁵

4. Results and Discussion

4.1. Adsorption and Desorption on Dry Coal. The experimental amounts of excess adsorbed CO₂ on dry coal at 298 and 318 K are shown in Figure 3. Because CO₂ is liquid above 63.5 atm at 298 K (subcritical temperature), the isotherm was measured only in the gas phase. As shown in Figure 3a, the amount of excess adsorbed CO₂ at 298 K increased steeply in the low-pressure range as the pressure increased. The adsorbed amount reached a constant value of approximately 1.41 mmol/g at higher than 30 atm and increased again near the saturation pressure.

The amount of excess adsorbed CO₂ at the subcritical temperature of 298 K was increased with pressure, which was same as the trend obtained at supercritical temperature of 318 K; however, the shape of the isotherm was different. The isotherm at 318 K showed an asymptotic increase of 50 atm, and it increased thereafter up to near the critical pressure. Even though the adsorbed amount at 318 K was lower than that at 298 K in the gas phase, the difference became negligible at the phase transition region from the subcritical to the supercritical condition. After passing the maximum excess adsorbed amount (1.5 mmol/g) near 75 atm, the isotherm decreased smoothly with an increase in pressure. The isotherm then showed a steep decrease around 100 atm, after which it decreased slightly again with increasing pressure.

The desorption isotherm at 318 K was obtained from depressurization conditions after the adsorption experiment. The change in adsorbed CO₂ was almost negligible from 150 to 100 atm. The isotherm then increased steeply with a decrease in pressure, and a crossover in the adsorption isotherm occurred around the critical point. After the critical point, the isotherm showed a convex shape according to pressure. Therefore, the maximum amount of CO₂ adsorbed in the desorption isotherm moved to the subcritical condition and was observed at around 40 atm (1.6 mmol/g), which was much different from the results of the adsorption isotherm.

Due to this hysteresis, the excess amount of adsorbed CO₂ from the desorption isotherm was higher than that of the

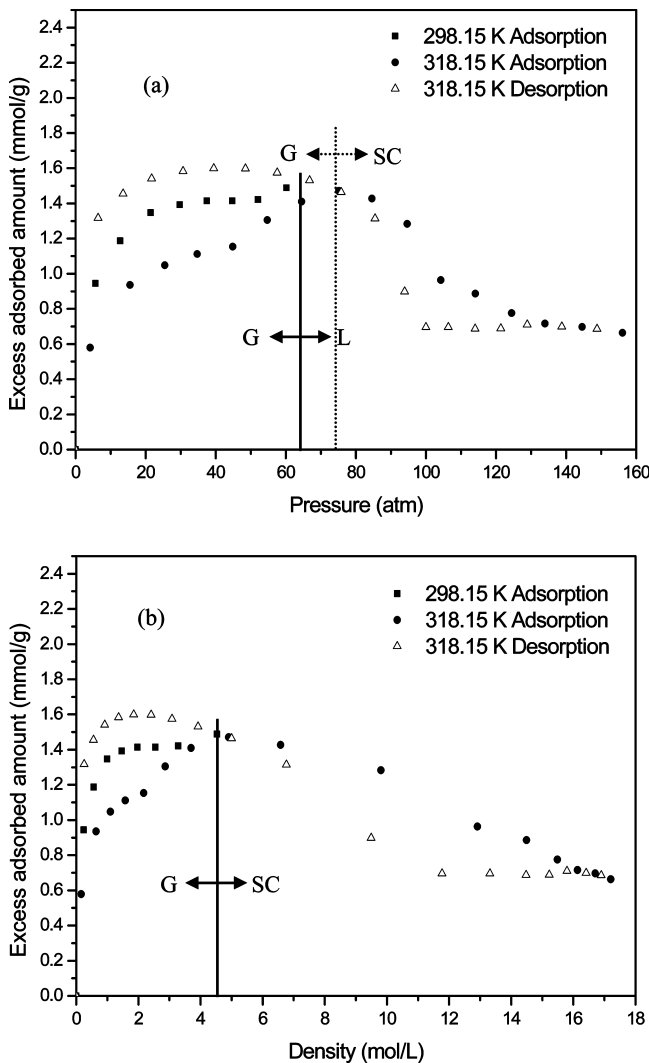


Figure 3. Adsorption and desorption of CO₂ on dry coal at 298 and 318 K with respect to pressure (a) and density (b).

adsorption isotherm in the gas phase. Conversely, the trend was opposite in the supercritical phase. It should be noted that the difference between the adsorption and desorption isotherms in the gas phase was almost 2 times higher than that in the supercritical phase with respect to CO₂ pressure in Figure 3a. On the other hand, in the CO₂ density variation, the opposite result was observed in Figure 3b because the CO₂ density is significantly changed in the critical region. Furthermore, the desorption isotherm at 318 K was greater than that at 298 K in the gas phase. This implied that the adsorbed CO₂ on coal was relatively stable even though the stored CO₂ in the coal seams was depressurized from the supercritical to the subcritical conditions. Furthermore, the desorption isotherm at 318 K was greater than the adsorption isotherm at 298 K in the gas phase.

The nonlinear decrease of excess CO₂ adsorption in the high-pressure range was due to the nonlinearity of the relationship between CO₂ density and pressure. Figure 3b shows the effect of CO₂ density on the excess amount of adsorbed CO₂. The isotherm at 298 K showed a shape similar to that in Figure 3a; however, the isotherm at 318 K increased almost linearly up to the critical density region after a steep increase in the low-density region. After passing the critical density, the isotherm decreased almost linearly. On the other hand, the linearity of the isotherm with density was not observed in the desorption curve, and the isotherm shape was similar to that in Figure 3a.

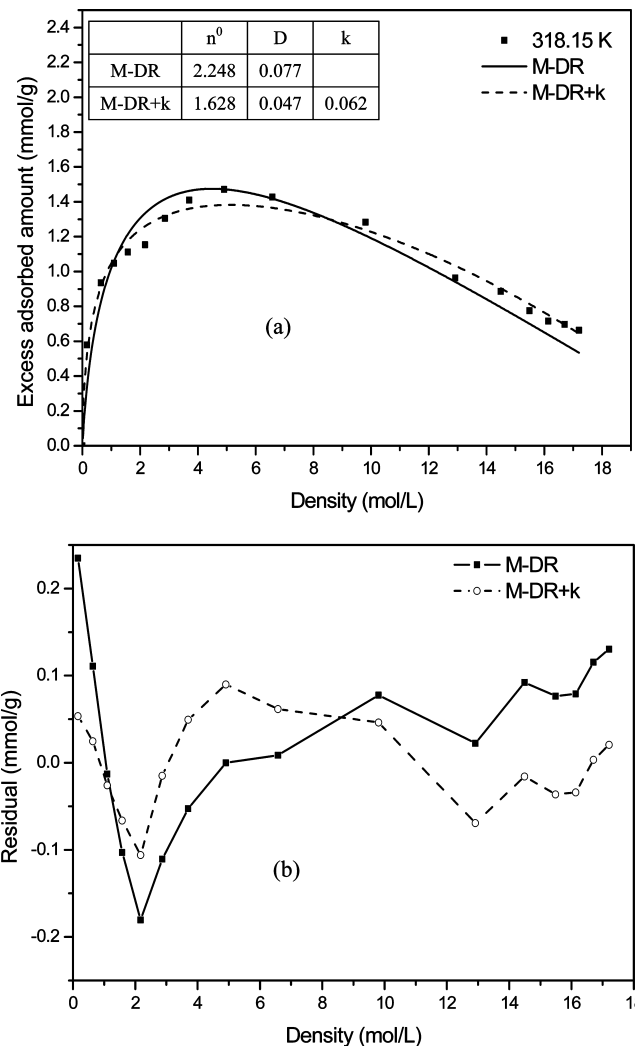


Figure 4. Prediction of CO₂ adsorption on dry coal at 318 K: fitted by M-DR and M-DR+k models (a) and their residuals (b).

And the pressure range (88–105 atm), which showed a sharp decrease in the adsorption and desorption isotherms, corresponded to the region of significant CO₂ density change.

The predicted results and fitting residuals according to the M-DR and M-DR+k models are shown in Figure 4a,b, respectively. Both the M-DR and M-DR+k models represented the experimental data reasonably well. The parameter value, n⁰ = 1.628 mmol/g, which was the saturated adsorption capacity in the M-DR+k model, was very close to the experimental result (maximum value 1.5 mmol/g), whereas the n⁰ value of the M-DR equation was much higher. In addition, the M-DR+k model showed a smaller deviation (± 0.1 mmol/g) from the experimental data compared to that of the M-DR model (± 0.2 mmol/g), as shown in Figure 4b. This implied that the M-DR+k model, which included the additive swelling term, fitted the data slightly better than did the M-DR model.

4.2. Swelling of Dry Coal. In this study, the swelling of coal was measured at the conditions of adsorption, desorption, and readsorption of CO₂. The volume percent of swelling by CO₂ adsorption is shown in Figure 5. During the adsorption step in the gas phase, the volume of coal increased. After the volume change reached a maximum of approximately 1.37% at 135 atm, it remained almost constant with further increases in pressure.

During the desorption step, the volume swelling percent was similar to that of the adsorption step in the supercritical region

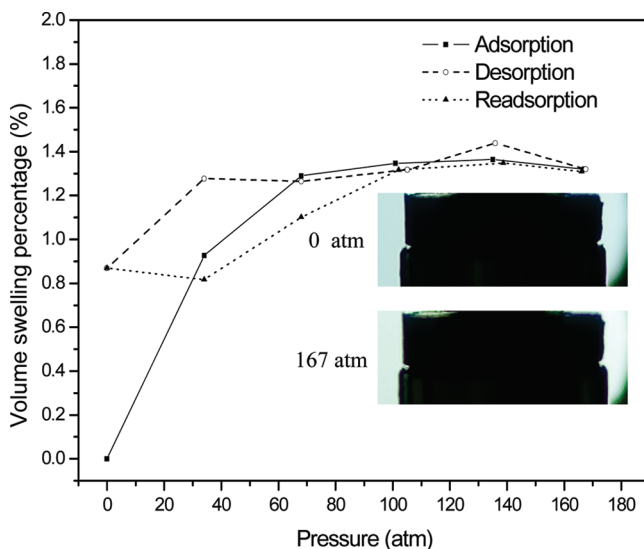


Figure 5. Volume swelling change of dry coal by CO_2 adsorption at 318 K.

after a small volume increase (1.44%). Furthermore, it remained almost constant around 30 atm. It should be noted that the pressure coincided with the pressure of the maximum adsorbed amount in the desorption isotherm, as shown in Figure 3a. Through further depressurization, the swelling percent decreased steeply. Furthermore, after applying a vacuum to the system for longer than 20 h, the coal volume did not return to its original size. It has been contradictorily reported that the swelling of bituminous coal is reversible.¹³

If the pressure of CO_2 stored in the coal seam was decreased by stabilization and expansion, an additional amount of CO_2 may be supplied. In this study, after the desorption swelling experiment, the readorption swelling by repressurization was measured. The readorption swelling curve decreased slightly with pressure. Then it showed an increase that was similar to the trend seen in the adsorption-swelling curve of virgin coal.

Figure 5 shows the trajectory of coal swelling in the gas phase during the adsorption, desorption, and readorption steps. Coal swelling was almost reversible in the supercritical phase during all pressure steps, and the maximum swelling of coal was observed in the supercritical region. However, the swelled coal could not return to its original volume during the desorption step even though vacuum was applied to the system. During the readorption step, the coal swelling showed a similar percentage variation to its virgin coal.

The maximum volume swelling percent in this study was lower than those reported in other studies for bituminous coals: nearly 1.9%,¹³ about 3.8%,¹⁴ and about 4% at 318 K.⁹ The difference from the published results may be a result of differing coal compositions. Moreover, because the coal used in this study was anthracite coal with a high amount of ash (30.66 wt %), less volume expansion by CO_2 adsorption was expected.

After the experimental data were corrected for the swelling percent of coal, the M-DR-k model was applied to the result in Figure 6. The contribution of swelling to the excess amount of adsorbed CO_2 was small in the gas phase, while it became significant in the supercritical region. For example, the excess amount of adsorbed CO_2 increased by 16.6% at a density of 17.2 mol/L (149 atm) after accounting for swelling. The parameter n^0 (1.522 mmol/g) from the M-DR+K equation was closer to the experimental result than was the result in Figure 4a. However, the residual analysis in Figure 6b showed small differences with and without swelling.

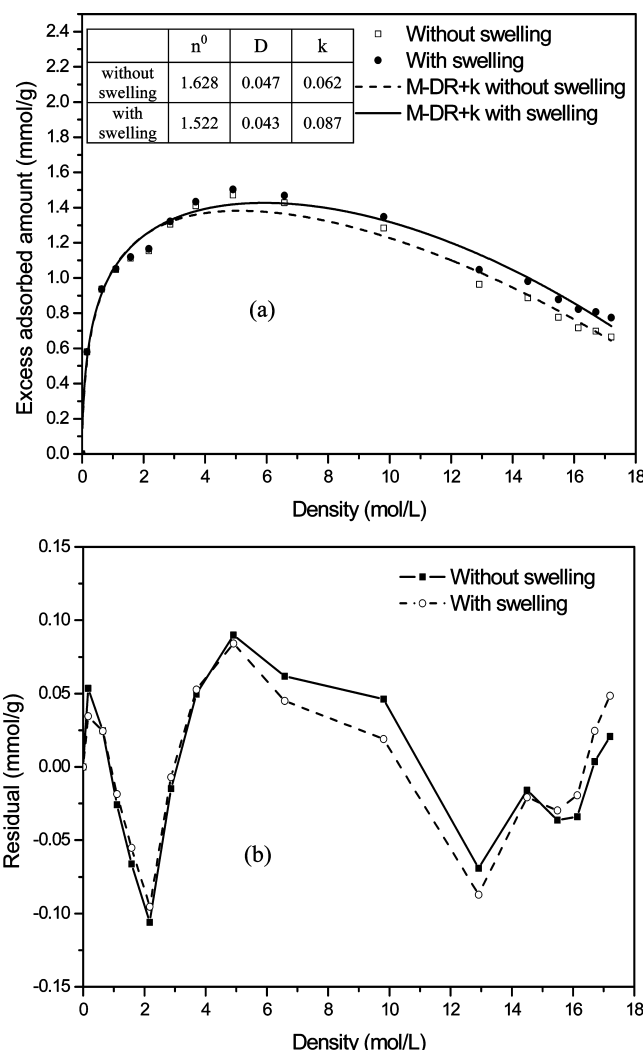


Figure 6. Effect of coal swelling on CO_2 excess adsorbed amount: fitted by M-DR+k model (a) and its residual (b).

4.3. Adsorption and Desorption on Wet Coal. The limiting moisture content on coal depends on the rank of the coal and the sorbate gas. It was reported that three bituminous coals were studied in the range 0.9–8.5% moisture, which corresponded approximately to the equilibrium moisture that would be attained by exposing the coal to about 40–80% RH.²⁰ In this study, the moisture content of the prepared wet coal was 3.64 wt %.

The adsorption and desorption isotherms of CO_2 on wet coal (3.64%) at 318 K were compared to those on dry coal, and the results are shown in Figure 7. At first, CO_2 adsorption showed an almost linear increase in the excess amount of adsorbed CO_2 (1.35 mmol/g) over the critical pressure. It then decreased sharply in the range 88–105 atm (Figure 7a), which was quite different from the adsorption isotherm of dry coal. After the sharp decrease, the excess amount of adsorbed CO_2 began to decrease smoothly. The adsorbed amount of CO_2 on wet coal was lower than that on dry coal in the experimental range except at the maximum excess adsorbed amount, which showed almost the same adsorbed amount with dry coal at the same temperature and pressure. Especially, the difference in the excess amount of adsorbed CO_2 between the dry and wet coals was more significant in the high supercritical pressure range (>100 atm). In addition, the maximum excess adsorbed amount in the wet coal was shifted to a higher pressure compared to the result for dry coal.

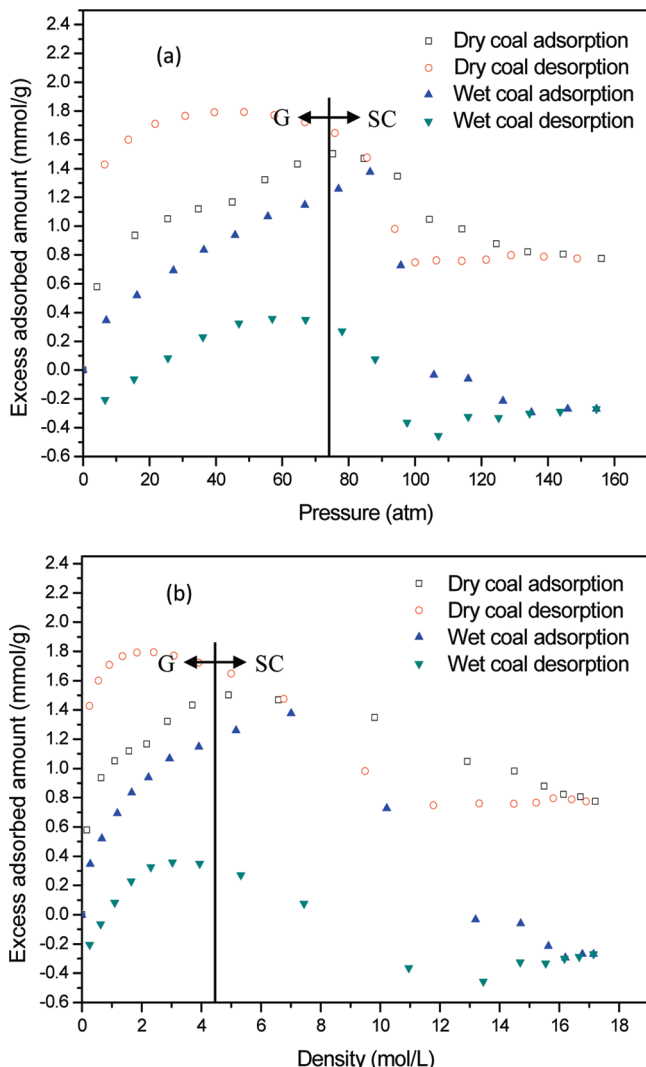


Figure 7. Comparison of adsorption and desorption of CO₂ between dry coal and wet coal (3.64%) at 318 K with respect to pressure (a) and density (b).

Figure 7b shows the excess amount of adsorbed CO₂ with respect to density. The excess adsorbed amount of CO₂ on wet coal in the gas phase showed a significant nonlinear increase with density, even though the adsorbed amount was smaller. In addition, the pressure range (88–105 atm), which showed a sharp decrease in the adsorbed amount (Figure 7a), corresponded to the region of significant density change in Figure 7b. The desorption isotherm of CO₂ on wet coal showed a hysteresis similar to that of the dry coal result. However, because isotherm crossover was not observed, the desorption isotherm was lower than the adsorption isotherm in the experimental range. The desorption isotherm remained nearly constant by 115 atm until it increased with a decrease in pressure after decreasing at the boundary of the significant density change region (Figure 7b). After showing a maximum value (0.39 mmol/g at 60 atm) in the gas phase, the adsorbed amount decreased nonlinearly with pressure. The difference in the adsorbed amount between the adsorption and desorption isotherms of the wet coal was much more significant than that of the dry coal, especially in the supercritical region.

In Figure 7, a negative amount of excess adsorbed CO₂ was found in the high supercritical pressure ranges of the adsorption/desorption isotherms. According to the definition of excess

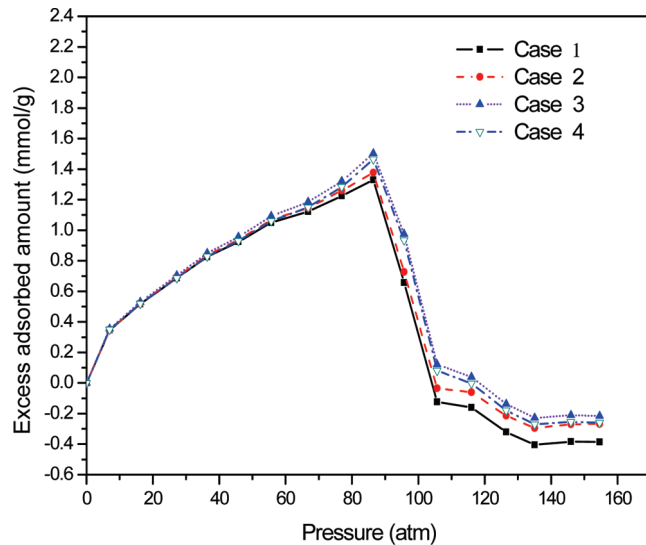


Figure 8. Effect of water in wet coal on CO₂ adsorption. Case 1: raw data. Case 2: considering coal swelling only. Case 3: considering coal swelling and water loss from the solid phase. Case 4: considering coal swelling, water loss, and absorption of CO₂ in the aqueous phase.

adsorbed CO₂, the density of the excess adsorbed phase should be lower than that of the supercritical fluid phase. Such experimental phenomena were observed in other reports for bituminous coal.^{26–28} In addition, the result agreed with the reported result that wet coal has a significantly lower maximum sorption capacity for CO₂ than does dry coal.^{2,20}

Compressed CO₂ could leach water from the coal;²¹ therefore, water in the bulk CO₂ fluid can cause an appreciable change in fluid density. In Figure 7, the CO₂ density could also be affected by the dissolved water vapor in the wet coal experiment because of the mutual dissolutions of CO₂ and H₂O in the fluid (gas or supercritical fluid) and aqueous phases. In this study, each component fraction in both phases was calculated using GSM-Gem, version 1.10 (Colorado School of Mines).²⁹ It was assumed that there were only two phases in the adsorption cell, the aqueous phase and the fluid phase. Because the water pressure in the fluid phase is subtracted from the system pressure change, the excess adsorbed amount should be increased compared to the experimental result. In addition, if the dissolved amount of CO₂ in the aqueous phase is excluded from the adsorbed amount, the level of excess adsorbed amount decreases.

The modified adsorption isotherm on the wet coal through the thermodynamic calculation is presented in Figure 8. Case 1 presents the raw data, and case 2 contains only the effect of swelling on CO₂ sorption. Case 3 implies the effects of swelling as well as water loss from the coal by the dissolution in CO₂ on CO₂ sorption. In case 4, the dissolution of CO₂ in water is added to case 3. Because the water dissolution in the CO₂ phase increased with pressure, the correction for the excess amount of adsorbed CO₂ was noticeable in the supercritical region. Then, the increase in the excess amount of adsorbed CO₂ of 15% at 154 atm was found. On the other hand, the change in the amount of adsorbed CO₂ in the gas phase was negligible. When the CO₂ absorption amount in water was excluded from this result, the change in the excess amount of adsorbed CO₂ was relatively small because the amount of water in the coal was small.

In addition to the effects of water vapor and CO₂ absorption on the isotherm, the changes in the coal physical properties before and after the wet coal experiments may also have affected the experimental results. Therefore, the experimented coal structure was analyzed.

TABLE 2: BET Results of Fresh Coal and Coals after Dry and Wet Experiments

	properties	fresh coal	after dry experiment	after wet experiment
surface area (m^2/g)	BET	5.65	7.09	3.25
	Langmuir	7.72	9.66	4.32
	t-plot micropore	2.3	3	2.96
	t-plot external	3.36	4.09	0.3
	BJH adsorption cumulative	2.57	3.28	1.1
	BJH desorption cumulative	2.55	2.73	1.92
	t-plot micropore	0.001	0.0013	0.0013
	BJH adsorption cumulative	0.015	0.015	0.011
	BJH desorption cumulative	0.014	0.013	0.011
	BJH adsorption average	24.02	17.77	40.49
pore volume (cm^3/g)	BJH desorption average	22.14	19.02	23.63
pore diameter (nm)	BJH adsorption average			
	BJH desorption average			

4.4. Coal Pore Changes Due to CO_2 Adsorption. Fresh coal and the coal that resulted after the dry and wet experiments were analyzed by BET, and the results were listed in Table 2. Compared to the fresh coal, the surface area of the coal used in the dry experiment increased, while its pore diameter decreased slightly. The change in pore volume was negligible. However, the pore structure on wet coal was observed in Table 2 after the wet experiment. The coal surface area decreased significantly, the pore volume decreased slightly, and the pore diameter increased, compared to fresh coal.

Such changes in surface areas in the dry and wet coals coincided with the behaviors of the desorption isotherm of each coal. As seen in Figure 5, the coal swollen by CO_2 adsorption at high pressure could not return to its original volume; therefore, the swelling of dry coal naturally led to pore contraction and an increase in surface area. On the contrary, it was expected that water in the coal contributed to a certain level of the pore breaking in the coal due to water compression by high pressure CO_2 . As shown in Figure 8, the coal swelling gave a significant effect on the excess adsorbed amount on the wet coal, especially in the supercritical region. Assuming coal swelling of about 5% in the wet condition, the negative values of excess adsorbed amounts in high supercritical region (from 100 to 154 atm) in Figure 7 became positive. Therefore, the large difference between adsorption and desorption isotherms in the wet coal may stem from water effect and coal structure change. This implied that the structural changes in coal might work as one of the key safety factors in CO_2 storage in wet coal seams.

5. Conclusions

The adsorption and desorption characteristics of CO_2 on dry and wet (3.64 wt %) coals (Kyungdong, anthracite coal) were measured using a static volumetric method from subcritical to supercritical conditions (298 and 318 K, and up to 150 atm). The effects of coal swelling on CO_2 adsorption, as well as the effects of water in the gas and liquid phases, were studied. The adsorption of CO_2 was more favorable at low temperature and dry coal than at high temperature and wet coal. A large difference in the isotherms between the dry and wet coals was observed in the high supercritical region (>100 atm). In the case of the dry coal, the adsorption isotherm was higher than the desorption isotherm in the supercritical condition; however, the opposite result was observed in the subcritical condition. Crossover of the two isotherms occurred near the critical region, and the maximum amount of adsorbed CO_2 was shifted from near the critical point to the subcritical region in the desorption isotherm. In the wet coal, the desorption isotherm was always lower than the adsorption isotherm. In addition, the difference between the adsorption and desorption isotherms in wet coal was higher than that in dry coal. Moreover, the difference

between both isotherms in the wet coal was most significant near the critical region, but the opposite result was observed for dry coal.

The maximum swelling of anthracite coal observed in the supercritical region, but the swelling was lower than that of bituminous coal. During desorption, coal shrinkage occurred mainly in the subcritical condition, and it was unable to shrink back to its original volume. Moreover, the swelling trend during readsorption was similar to adsorption swelling, and the hysteresis of coal swelling was only observed in the subcritical condition. In addition, the structure of wet coal was significantly affected by CO_2 adsorption at high pressure compared to the dry coal results. The effects of coal swelling and water in the gas/liquid phases on CO_2 adsorption should be considered to accurately estimate the adsorption amount, especially in the supercritical condition.

The stored CO_2 in coal seams can diffuse to other geological strata and leak to the surface of the earth. Both cases will lead to a depressurization of the stored CO_2 , and the capacity estimation using the adsorption isotherms will lead to a certain level of error. In dry coal seams, depressurization by leakage or expansion of stored CO_2 may not lead to significant problems in the coal seam due to the favorable desorption isotherm in the subcritical condition and the coal structural stability. However, in wet coal seams, leakage or expansion of stored CO_2 may lead to a serious loss of CO_2 adsorption capacity and coal pore structure. On the basis of these results, coal seams for CO_2 storage should be monitored for safety, as affected by the possible structural changes in the coal.

Acknowledgment. We gratefully acknowledge the financial support provided to this work by 21C Frontier Project (CDRS: 16-2008-00-012-00) from Ministry of Education, Science, and Technology, South Korea.

References and Notes

- Price J.; Smith, B. *Geologic storage of carbon dioxide: staying safely underground*; IEA Greenhouse Gas R&D program: Gloucestershire, U.K., 2008.
- Mazzotti, M.; Pini, R.; Storti, G. *J. Supercrit. Fluids* **2009**, *47*, 619.
- Pashin, J. C.; McIntyre, M. R. *Int. J. Coal Geol.* **2003**, *54*, 167.
- Ryu, Y. K.; Kim, K. L.; Lee, C. H. *Ind. Eng. Chem. Res.* **2000**, *39*, 2510.
- Zhou, Y.; Zhou, L. *Langmuir* **2009**, *25*, 13461.
- Kaneko, K. *Col. Surf. A* **1996**, *109*, 319.
- Day, S.; Duffy, G.; Sakurovs, R.; Weir, S. *Int. J. Greenhouse Gas Control* **2008**, *2*, 342.
- Sakurovs, R.; Day, S.; Weir, S.; Duffy, G. *Energy Fuels* **2007**, *21*, 992.
- Ottiger, S.; Pini, R.; Storti, G.; Mazzotti, M. *Adsorption* **2008**, *14*, 539.
- Larsen, J. W. *Int. J. Coal Geol.* **2004**, *57*, 63.
- Melnichenko, Y. B.; Radlinski, A. P.; Mastalerz, M.; Cheng, G.; Rupp, J. *Int. J. Coal Geol.* **2008**, *77*, 69.

- (12) Pan, Z.; Connell, L. D. *Int. J. Coal Geol.* **2007**, *69*, 243.
(13) Day, S.; Fry, R.; Sakurovs, R. *Int. J. Coal Geol.* **2008**, *74*, 41.
(14) Bae, Y. S.; Lee, C. H. *Carbon* **2004**, *43*, 95.
(15) Bae, Y. S.; Moon, J. H.; Ahn, H. W.; Lee, C. H. *Korean J. Chem. Eng.* **2004**, *21*, 712.
(16) Glandt, E. D. Klein; M. T. Edgar; T. F. *Introduction to chemical engineering thermodynamics*, 7th ed.; McGraw-Hill Education: New York, 2005.
(17) NIST, Thermophysical Properties of Fluid Systems. <http://webbook.nist.gov/chemistry/fluid/>, 2008.
(18) Bae, J. S.; Bhatia, S. K. *Energy Fuels* **2006**, *20*, 2599.
(19) Siemons, N.; Busch, A. *Int. J. Coal Geol.* **2007**, *69*, 229.
(20) Day, S.; Sakurovs, R.; Weir, S. *Int. J. Coal Geol.* **2008**, *74*, 203.
(21) Fitzgerald, J. E.; Sudibandriyo, M.; Pan, Z.; Robinson, R. L., Jr.; Gasem, K. A. M. *Carbon* **2003**, *41*, 2203.
(22) Chen, J. H.; Wong, D. S. H.; Tan, C. S.; Subramanian, R.; Lira, C. T.; Orth, M. *Ind. Eng. Chem. Res.* **1997**, *36*, 2808.
(23) Fitzgerald, J. E.; Pan, Z.; Sudibandriyo, M.; Robinson, R. L., Jr.; Gasem, K. A. M.; Reeves, S. *Fuel* **2005**, *84*, 2351.
(24) Ottiger, S.; Pini, R.; Storti, G.; Mazzotti, M. *Langmuir* **2008**, *24*, 9531.
(25) Zhou, L.; Bai, S.; Zhou, Y.; Yang, B. *Adsorption* **2002**, *8*, 79.
(26) Walker, P. L.; Verma, S. K.; Rivera-Utrilla, J.; Khan, M. R. *Fuel* **1988**, *67*, 719.
(27) Krooss, B. M.; van Bergen, F.; Gensterblum, Y.; Siemons, N.; Pagnier, H. J. M.; David, P. *Int. J. Coal Geol.* **2002**, *51*, 69.
(28) Goodman, A. L.; Busch, A.; Bustin, R. M.; Chikatamarla, L.; Day, S.; Duffy, G. J.; Fitzgerald, J. E.; Gasem, K. A. M.; Gensterblum, Y.; Hartman, C.; Jing, C.; Krooss, B. M.; Mohammed, S.; Pratt, T.; Robinson Jr., R. L.; Romanov, V.; Sakurovs, R.; Schroeder, K.; White, C. M. *Int. J. Coal Geo.* **2002**, *51*, 69.
(29) Sloan, E. D., Jr.; Carolyn A. Koh. CSMGem Hydrate Prediction Program, version 1.10; Colorado School of Mines: Golden, CO, 2007.

JP911712M